Water Research 128 (2018) 206–216

Contents lists available at ScienceDirect

Water Research

journal homepage: www.elsevier.com/locate/watres

Warming and eutrophication combine to restructure diatoms and dinoflagellates

Wupeng Xiao [a, b, 1], Xin Liu [a, b, 1], Andrew J. Irwin [c], Edward A. Laws [d], Lei Wang [a, b], Bingzhang Chen [e], Yang Zeng [a, b], Bangqin Huang [a, b, *]

[a] State Key Laboratory of Marine Environmental Science, Xiamen University, Xiamen, China
[b] Key Laboratory of Coastal and Wetland Ecosystems, Ministry of Education/Fujian Provincial Key Laboratory of Coastal Ecology and Environmental Studies, Xiamen University, Xiamen, China
[c] Department of Mathematics & Computer Science, Mount Allison University, Sackville, New Brunswick, Canada
[d] Department of Environmental Sciences, School of the Coast & Environment, Louisiana State University, Baton Rouge, LA, 70803, USA
[e] Ecosystem Dynamics Research Group, Research and Development Center for Global Change, Japan Agency for Marine-Earth Science and Technology, Yokohama, Japan

ARTICLE INFO

Article history:
Received 14 June 2017
Received in revised form
27 September 2017
Accepted 23 October 2017
Available online 24 October 2017

Keywords:
Diatoms
Dinoflagellates
Warming
Eutrophication
Generalized additive mixed models
The East China Sea

ABSTRACT

Temperature change and eutrophication are known to affect phytoplankton communities, but relatively little is known about the effects of interactions between simultaneous changes of temperature and nutrient loading in coastal ecosystems. Here we show that such interaction is key in driving diatom-dinoflagellate dynamics in the East China Sea. Diatoms and dinoflagellates responded differently to temperature, nutrient concentrations and ratios, and their interactions. Diatoms preferred lower temperature and higher nutrient concentrations, while dinoflagellates were less sensitive to temperature and nutrient concentrations, but tended to prevail at low phosphorus and high N:P ratio conditions. These different traits of diatoms and dinoflagellates resulted in the fact that both the effect of warming resulting in nutrients decline as a consequence of increasing stratification and the effect of increasing terrestrial nutrient input as a result of eutrophication might promote dinoflagellates over diatoms. We predict that conservative forecasts of environmental change by the year 2100 are likely to result in the decrease of diatoms in 60% and the increase of dinoflagellates in 70% of the surface water of the East China Sea, and project that mean diatoms should decrease by 19% while mean dinoflagellates should increase by 60% in the surface water of the coastal East China Sea. This analysis is based on a series of statistical niche models of the consequences of multiple environmental changes on diatom and dinoflagellate biomass in the East China Sea based on 2815 samples randomly collected from 23 cruises spanning 14 years (2002–2015). Our findings reveal that dinoflagellate blooms will be more frequent and intense, which will affect coastal ecosystem functioning.

1. Introduction

Anthropogenic eutrophication and global warming have dramatic impacts on marine phytoplankton and are likely to continue for many centuries (Doney et al., 2012; Hallegraeff, 2010; Karl and Trenberth, 2003). Eutrophication is a major problem in many coastal ecosystems and has resulted in large phytoplankton blooms and the expansion of low-oxygen dead zones (Anderson et al., 2002; Edwards et al., 2006). Warming affects phytoplankton in two fundamentally different ways: directly through the effect of warming on metabolic rates and indirectly through physical mixing, which affects nutrient availability (Lewandowska et al., 2014). Simultaneous warming and eutrophication will have complex consequences because of interactions between the processes that are driven by nutrient supply and metabolic rates. There is accumulating evidence that the intensity of the response differs considerably across taxa; these changes may therefore cause a shift in phytoplankton community structure (Barton et al., 2016; Edwards and Richardson, 2004; Irwin et al., 2012; Wells et al.,

* Corresponding author. State Key Laboratory of Marine Environmental Science, Xiamen University, Xiamen, China.
E-mail address: bqhuang@xmu.edu.cn (B. Huang).
[1] These authors contributed equally to this work.

https://doi.org/10.1016/j.watres.2017.10.051
0043-1354/

2015; Xie et al., 2015).

Within the phytoplankton community, the consequences for diatoms and dinoflagellates are a major concern because these taxa play key roles in ecosystem processes and form the basis of many aquatic food webs (Agusti et al., 2014; Menden-Deuer and Lessard, 2000). Diatoms and dinoflagellates are two typical groups that form harmful phytoplankton blooms, which can adversely affect human health as well as marine fisheries and aquaculture (Anderson et al., 2002; Moore et al., 2008). In fact, dinoflagellates and diatoms account for 75% and 5% of all harmful phytoplankton species, respectively (Smayda and Reynolds, 2003). Various theoretical arguments based on laboratory experiments and field studies suggest that phytoplankton bloom dynamics and habitat preferences can be described in terms of nutrient availability, degree of mixing, and/or nutrient/resource ratios (Margalef, 1977; Reynolds, 1987; Smayda and Reynolds, 2001, 2003; Tilman, 1977). All of these factors are closely correlated with coastal eutrophication and surface layer warming. While numerous studies have shown that the relative abundance of diatoms and dinoflagellates varies in response to regional climate warming, contrasting results can be obtained (Hinder et al., 2012; Leterme et al., 2005, 2006; Xie et al., 2015), because the net effect of warming depends on other environmental changes. Quantitative predictive models that consider the effects of temperature and nutrient interactions on the concentrations of diatoms and dinoflagellates are still in their infancy for the lack of sufficient real-time data (Glibert et al., 2010; Moore et al., 2008; Wells et al., 2015). In this study we developed a series of statistical niche models to explore the existing relationships between the diatom and dinoflagellate biomass and environmental factors, and to project the biomass of diatoms and dinoflagellates in response to future environmental changes using an extensive dataset of coastal phytoplankton community composition and water quality from the entire euphotic zone in the East China Sea (ECS), a region that is affected by both eutrophication and warming and that is important to biogeochemical cycles and fisheries.

Previous studies have demonstrated that diatoms are dominant during much of the year in the ECS, but dinoflagellates become important during late spring blooms (Guo et al., 2014). Long-term studies have found that the relative biomass of diatoms compared to dinoflagellates has decreased during a time of increasing coastal eutrophication (Jiang et al., 2014; Tang et al., 2006; Zhou et al., 2008). Our earlier work revealed that differences in the responses of diatoms and dinoflagellates to temperature may result in the earlier occurrence of dinoflagellate blooms (Liu et al., 2016). Here, we further propose that warming combined with eutrophication may have a great impact on the dynamics of diatoms and dinoflagellates in the ECS.

2. Materials and methods

2.1. Data sources

Available material makes the ECS an ideal region for studying the effects of environmental changes on phytoplankton community dynamics (see SI 1). We conducted 23 cruises spanning 14 years (2002–2015) and obtained 2815 pigment samples in the ECS (Fig. 1, Table S1). The cruises took place in all four seasons and during most months of the year. Stations were located irregularly in space and were not all the same between cruises. Data density was greatest near the Changjiang River estuary and adjacent coastal waters (Fig. 1).

Temperature, salinity and water pressure were determined at every station from casts of a Sea Bird CTD fitted with a Sea Tech fluorometer. Using Niskin bottles attached on the CTD rosette system, seawater samples were taken in the euphotic zone

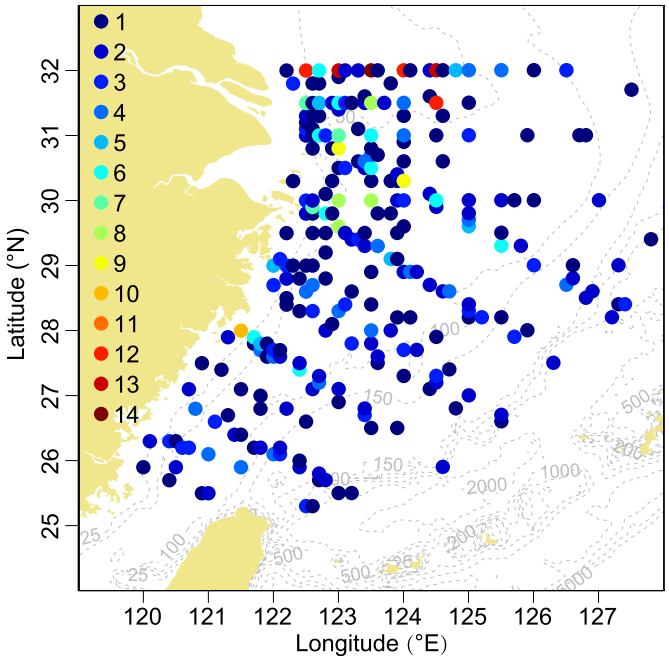

Fig. 1. Sampling stations from 23 cruises in the East China Sea from 2002 to 2015. Symbol color represents the number of overlapping stations between the cruises. (For interpretation of the references to colur in this figure legend, the reader is referred to the web version of this article.)

(≤150 m) from at least three layers: the surface water (≤5 m), the subsurface chlorophyll *a* (Chl*a*) maximum, and the bottom of the euphotic zone. The euphotic zone was defined as the water column down to the depth at which the downward photosynthetically active radiation (PAR) was 1% of the value just below the surface. PAR was made using a free-fall spectroradiometer (SPMR, Satlantic) just prior to water sampling. Nutrient concentrations were determined by professional laboratories (Han et al., 2012; Liu et al., 2016). To avoid issues with detection limits, nutrient concentrations below the detection limit were deemed as the value of detection limit. Samples for phytoplankton pigment analysis were collected at every station on all cruises. Pigment concentrations were measured by high performance liquid chromatography (HPLC) following the method presented by Furuya et al. (2003) and are reported in detail by Liu et al. (2012).

The long-term sea surface Chl*a* (mg m^{-3}) from August 1997 to January 2015 was extracted from multiple-satellite products (AVHRR, QuikSCAT, SeaWiFS and MODIS/Aqua). The resolutions of these four databases were 0.044, 0.25, 0.1 and 0.05° respectively.

2.2. Generalized additive mixed models

To explore how temperature and nutrients influence the dynamics of diatoms and dinoflagellates, we developed a series of generalized additive mixed models (GAMMs), which are an extension of GAMs (see SI 2) (Wood, 2006; Zuur et al., 2009). Fucoxanthin (C_f) and peridinin (C_p) concentration were used as response variables. Fucoxanthin and peridinin are the diagnostic photosynthetic pigments of diatoms and autotrophic peridinin-containing dinoflagellates, respectively (Roy et al., 2011). Phytoplankton community structure determined from diagnostic pigment concentration is widely used because it is easier to obtain high resolution data relative to microscopic and molecular methods (Peloquin et al., 2013).

Temperature (°C), salinity (psu), nitrate + nitrite (NO_x, μmol

L^{-1}), soluble reactive phosphorus (PO_4, μmol L^{-1}) and the ratio of NO_x and PO_4 (N:P) were taken as potential environmental explanatory variables. Silicate (SiO_3, μmol L^{-1}) was not incorporated into the models for reasons that silicate is usually not limiting in the ECS (Guo et al., 2014; Zhou et al., 2008) and that its effect covaried with NO_x and/or PO_4 during our initial test. TChl*a* (the sum of Chl*a* plus divinyl chlorophyll *a*, ng L^{-1}), geographic and temporal parameters (longitude, latitude, depth, month) were incorporated into the models as proxies for some missing parameters driving phytoplankton dynamics (e.g., grazing, light). In order to account for the potential influence of the different measuring instruments, we added a nominal variable representing the measurement effect for each group of cruises (Table S1). Of all these variables, we focus on the results of temperature and nutrient parameters, which are most likely to change in the future.

Before modeling, we used Cleveland dot plots and boxplots to check for potential outliers in both response and explanatory variables and used pairplots to check for collinearity between the explanatory variables. After quality control we had 2809 observations of C_f and 1998 observations of C_p remaining. C_f, C_p, TChl*a*, NO_x, PO_4 and N:P ratio were ln transformed (Figs. S1 and S2, see SI 2).

To reduce collinearity, we built a set of models (Models F1–F3, P1–P3) that use NO_x as the metric of nutrient availability, a similar set of models (Models F4–F5, P4–P5) that use PO_4 for comparison, and a set of models that use the N:P ratio instead (Models F6–F7, P6–P7), among which a set of models (Models F3, P3, F5, P5, F6, P6) treated nutrient parameters as independent variables and another set of models (Models F1–F2, P1–P2, F4, P4, F7, P7) assumed interactions between temperature and nutrients (Table S2).

The model without interaction between temperature and nutrient (NO_x, PO_4, or N:P) was:

$$\begin{aligned}\ln Y = {} & \alpha + a_i + s(\text{longitude},\ \text{latitude}) + s(\text{temperature}) \\ & + s(\text{nutrient}) + s(\text{TChl}a) + s(\text{salinity}) + s(\text{depth}) \\ & + s(\text{month}) + \varepsilon \end{aligned} \quad (1)$$

While the model with temperature and nutrient interaction was:

$$\begin{aligned}\ln Y = {} & \alpha + a_i + s(\text{longitude},\ \text{latitude}) \\ & + te(\text{temperature},\ \text{nutrient}) + s(\text{TChl}a) + s(\text{salinity}) \\ & + s(\text{depth}) + s(\text{month}) + \varepsilon \end{aligned} \quad (2)$$

where Y represents C_f or C_p and i denotes measuring instrument. The term α is a grand mean. The term a_i is a random intercept assumed to be normally distributed with mean 0 and variance σ_a^2, which allows for random variation around the intercept and reflects between measurement variability. The term $s(\cdot)$ indicates a one-dimensional nonlinear function based on cubic regression spline and $te(\cdot)$ a two dimensional effect based on tensor product spline. The two models are nested because *te*(temperature, nutrient) contains *s*(temperature), *s*(nutrient), and their interaction. The term ε represents within measurement variability, and it is assumed to independently, normally distributed with variance σ^2. Furthermore, the σ^2 is assumed allowing heterogeneity between months as the homogeneity assumption was violated along the month effect (Fig. S3, see SI 3).

2.3. Generalized linear models

To simulate the effect of interactions of temperature and nutrients on the relative biomass of diatoms and dinoflagellates, we formulated a more robust generalized linear model (GLM). In this model, only samples of the upper 15 m were used. The samples were divided into 64 bins on the basis of every 2.5 °C in temperature and every 1 interval in ln transformed PO_4 concentrations. The medians of each parameter in each bin were extracted instead of the raw data. After removing those bins with less than 3 samples, we had 37 available bins remaining.

We used the ratio of peridinin/fucoxanthin (C_p/C_f) instead of their absolute concentrations as the response variable. Temperature, NO_x and PO_4 concentrations were taken as the explanatory variables. The model was formulated as follows:

$$\begin{aligned} C_p \Big/ C_f = {} & \sum_{a=0}^{4}\sum_{b=0}^{4}\sum_{c=0}^{4}\beta_{abc}(\text{temperature})^a(NO_x)^b(PO_4)^c,\ a+b+c \\ & \le 4 \end{aligned} \quad (3)$$

which produced 25 independent variables (Table S4). The term β_{abc} is the coefficient of each variable. It will be the intercept when a, b and c equate zero at the same time. We assumed a *gamma* distribution with log-link function to keep the fitted ratio of C_p/C_f more than zero. Model optimization was based on the AIC value and the *t*-statistic, i.e., dropping the variables that did not reduce the AIC value significantly step by step, and dropping those variables that did not significantly correlated with C_p/C_f judged by the *t*-statistic.

Model simulations were conducted by assuming possible changes in temperature and nutrients concentration. The actual data showed the NO_x concentration was linearly correlated with the PO_4 concentration, but the slope was dependent on the PO_4 concentration (Fig. S4a). In addition, the N:P ratio was nonlinearly correlated with temperature (Fig. S4b). We took this into account by linking NO_x as the function of PO_4 and temperature. The model formation was built as follows:

$$\ln(NO_x) = \alpha + \beta_1 \times \ln(PO_4) + s(\text{temperature}) \quad (4)$$

where α is the intercept and β the slope of $\ln(PO_4)$. The s(temperature) term means a cubic regression spline for the temperature. The model accounted for 93% of the variance of logarithms of NO_x concentration. Then we calculate NO_x from PO_4 and temperature based on this equation.

All analyses were done using R in version 3.2.2 (R Development Core Team, 2016). The GAMMs and GAMs were fitted with the 'mgcv' (GAMs with GCV smoothness estimation and GAMMs by REML/ML (Wood, 2006)) package.

3. Results

3.1. Long-term variations of phytoplankton in the ECS

Long-term sea surface Chl*a* concentration in our study area from multiple-satellite products displayed a clear seasonal cycle in each year (Fig. 2a). The maximum in Chl*a* occurred in spring followed by another peak in summer. The magnitude of the spring algal bloom appeared to increase since 2000, except the last two years (Fig. 2a). Monthly averaged TChl*a* concentrations collected from our field observations matched well with satellite derived Chl*a* ($r = 0.55$, $p < 0.01$ after removing four observations with TChl*a* concentration greater than 2.5 mg m^{-3}) given the uncertainty of satellite data and irregularity of our sampling areas. The ratio of surface peridinin/fucoxanthin increased during the last 10 years (Fig. 2b). High fucoxanthin occurred in early spring and summer (Fig. S3a); high peridinin values were found in late spring and summer (Fig. S3b).

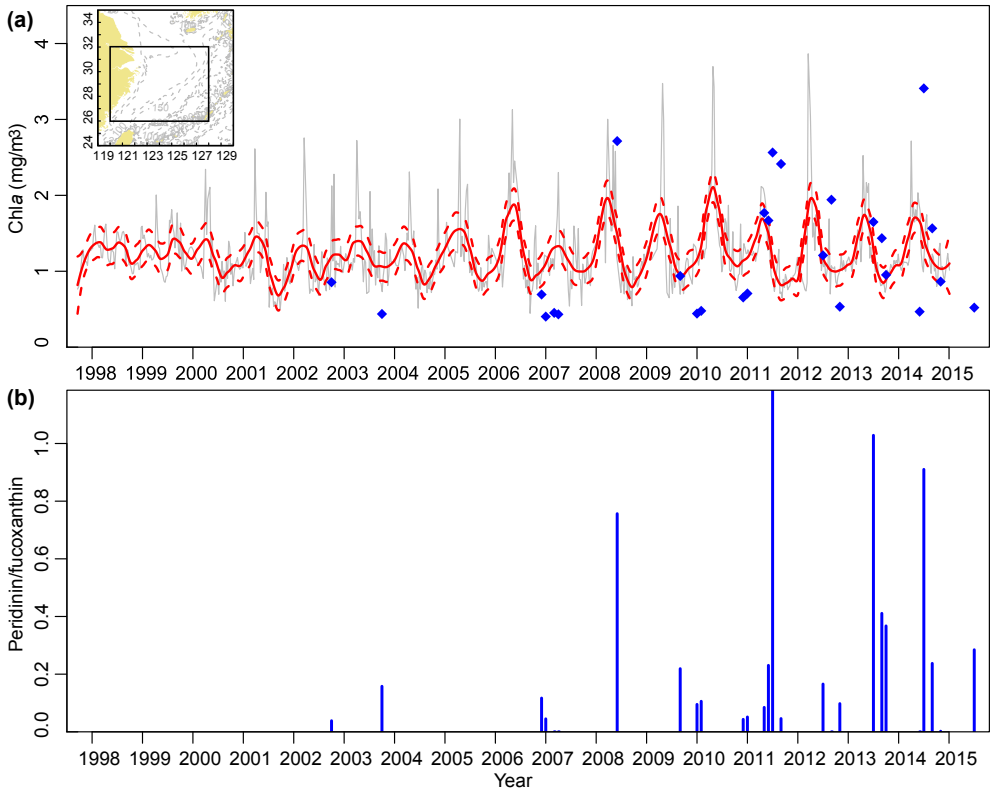

Fig. 2. Long-term variations of phytoplankton pigments. **a.** Long-term variations of surface Chl*a* concentration for an 8° × 6° region (120–128°N by 26–32°E) in the ECS. The grey line is the weekly averaged data obtained from the satellite; the red solid line produced by loses smoothing and the red dashed lines represent 95% confidence intervals; the blue diamonds are monthly averaged surface TChl*a* determined by HPLC during our field cruises. **b.** Ratio of monthly median surface peridinin and fucoxanthin concentrations. (For interpretation of the references to colour in this figure legend, the reader is referred to the web version of this article.)

3.2. Partial effects of temperature and nutrients on C_f and C_p

Temperature was significantly correlated with both C_f and C_p with different relationships (Fig. 3a and b). After keeping other parameters constant, the partial effect of temperature on C_f was significantly positive below ~24 °C and strongly negative above ~24 °C. There was a plateau of high C_f at temperatures of 20–24 °C (Fig. 3a). C_p was less sensitive to temperature than C_f (Fig. 3b). C_p was positively correlated with temperature in the approximate range 13–26 °C, insensitive to temperature at temperatures of 10–13 °C, and negatively correlated with temperature at temperatures of 26–30 °C (Fig. 3b). The optimum temperature for C_f was roughly 24 °C versus 26 °C for C_p, and the decline of C_f at temperatures exceeding 24 °C was much more precipitous than the analogous decline of C_p at temperatures exceeding 26 °C (Fig. 3a and b). These results suggest that peridinin-containing dinoflagellates are better able to tolerate high temperatures than fucoxanthin-containing phytoplankton.

Both C_f and C_p responded nonlinearly to nutrient concentrations (Fig. 3c–f). NO_x was positively correlated with C_f at NO_x concentrations less than ~6 μmol L^{-1} (Fig. 3c). C_p was positively correlated with NO_x at NO_x concentrations less than ~1 μmol L^{-1} but negatively correlated thereafter (Fig. 3d). When PO_4 was used as the independent variable instead of NO_x, its effect on C_f was qualitatively similar to that of NO_x; C_f and PO_4 were positively correlated at PO_4 concentrations below ~0.3 μmol L^{-1}, but there was no correlation at higher PO_4 concentrations (Fig. 3e). There was no highly significant correlation (*t*-test, $p = 0.2$) between PO_4 and C_p across the range of PO_4 concentrations in the database, ~0.01 μmol L^{-1} to ~2.7 μmol L^{-1} (Fig. 3f), the indication being that C_p may not be sensitive to phosphate concentrations. These trends also show that optimal NO_x and PO_4 concentrations for C_f are much higher than those for C_p, the clear indication being that peridinin-containing dinoflagellates tend to dominate at nutrient concentrations lower than those associated with fucoxanthin-containing phytoplankton dominance.

C_f and C_p have an opposite relationship with N:P ratio (Fig. 3g and h). The relationship between N:P and C_f was unimodal, with maximum C_f values at N:P ratio of ~16 (Fig. 3g). The correlation between N:P and C_p was positive across the observed range of N:P ratios (0.2–300), but there was a local minimum at a N:P of ~16 (Fig. 3h).

3.3. Combined effects of temperature and nutrients on C_f and C_p

The interactions between temperature and nutrient concentrations were significantly correlated with both C_f and C_p ($p < 0.0001$, Table S3) and inclusion of these interactions produced statistically better results than the models assuming no interaction (Table S2, see F2 (P2) versus F3 (P3), F4 (P4) versus F5 (P5), and F6 (P6) versus F7 (P7)). The nature of the interaction between temperature and NO_x was clear in the case of C_f (Fig. 4a). The negative correlation between C_f and temperature estimated from the partial temperature effect (Fig. 3a) for temperatures above 20 °C was apparent, but the magnitude of the slope was negatively correlated with NO_x concentrations (Fig. 4a). The implication is that fucoxanthin-containing phytoplankton are better able to tolerate supraoptimal temperatures at relatively high NO_x concentrations. The response of C_p to the interaction of temperature and NO_x, however, was rather complex (Fig. 4d). C_p remained relatively low but with two

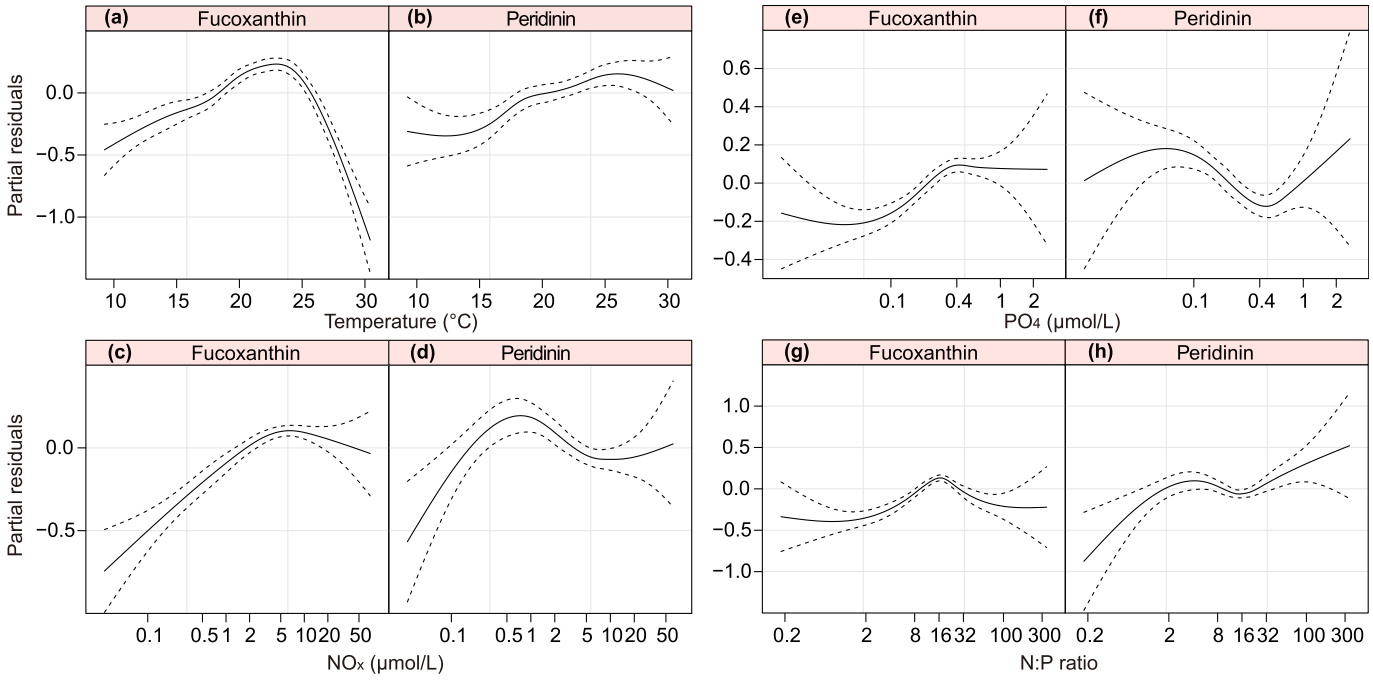

Fig. 3. Partial effects of temperature and nutrient concentrations or ratios on logarithms of fucoxanthin and peridinin. (**a, c**), (**b, d**), (**e**), (**f**), (**g**) and (**h**) are results produced by models F3, P3, F5, P5, F7 and P7, respectively (Table S2). The solid line is the smoother and the dashed lines 95% confidence bands. The partial temperature effect on fucoxanthin and peridinin was qualitatively independent of whether NO_x, PO_4, or N:P ratio was used as the metric of nutrient availability in the models.

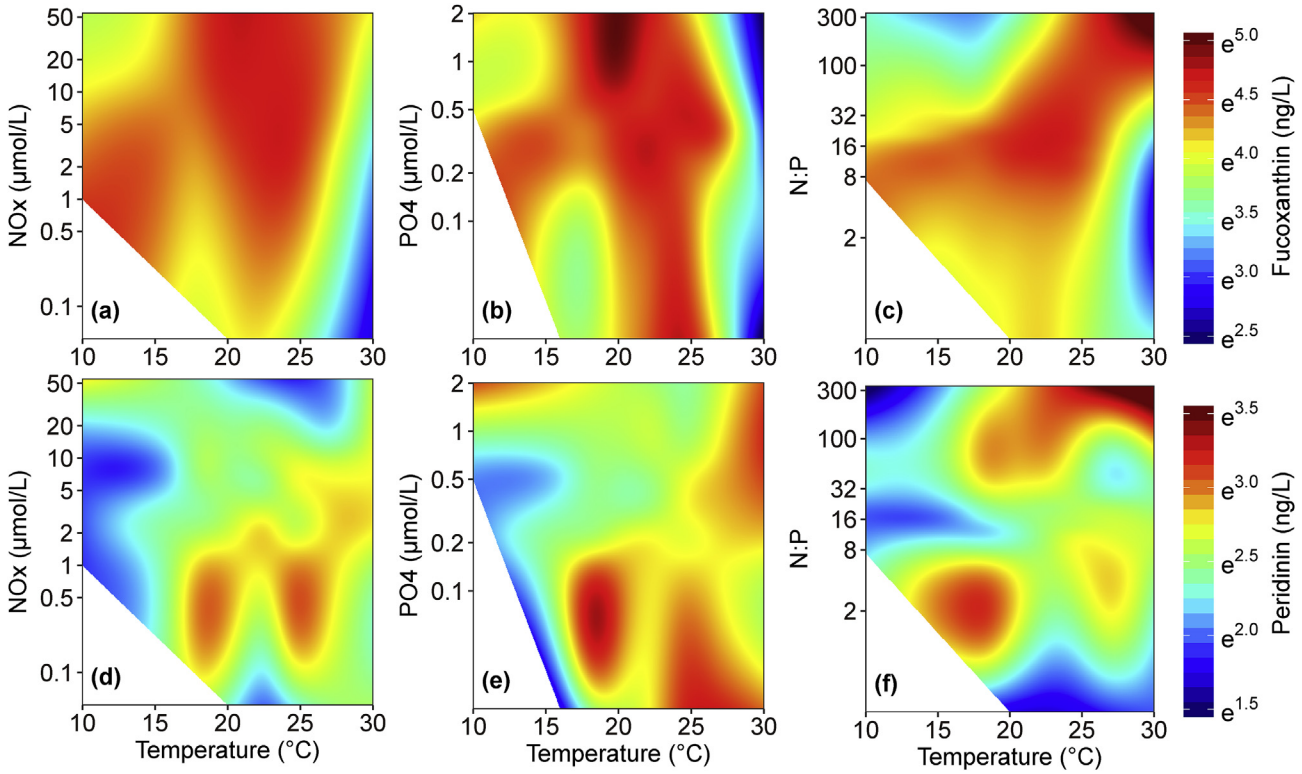

Fig. 4. Combined effects of temperature and nutrient concentrations or ratios on fucoxanthin and peridinin. **a**–**f** are results produced by models F2, F4, F6, P2, P4 and P6, respectively (Table S2). White areas in the lower-left corner of each panel represent there are few observations to support credible estimations.

obvious peaks at temperatures of ~18 °C and ~25 °C, and the corresponding NO_x concentrations were both around 1 μmol L^{-1}, which is consistent with the partial NO_x effect (Fig. 3d).

The interactive model of the effects of temperature and PO_4 on C_f produced results qualitatively similar to the results of the interactive model with temperature and NO_x, although the response

surface was more complex (Fig. 4b). The effect of interactions between temperature and PO_4 on C_p (Fig. 4e) was quite different from that of temperature and NO_x. The model results showed high C_p values in some regions where C_f values were low (Fig. 4b,e). At the lowest PO_4 concentrations, C_p increased dramatically with increasing temperature. At intermediate PO_4 concentrations, there was a maximum C_p at a temperature of ~18 °C; at higher PO_4 concentrations, C_p was relatively insensitive to temperature. The results of these models (Models P2, P4 and P6, Table S2) imply that the relationship between C_p and temperature depends on the PO_4 concentration (Fig. 4e).

Use of N:P and temperature as independent variables revealed relationships with C_f and C_p that were less complex than was the case when nutrient availability was quantified in terms of nutrient concentrations (Fig. 4c,f). The temperature-N:P models suggested that C_f would exceed $e^4 = 55$ under most conditions (Fig. 4c), whereas C_p exceeded $e^3 = 20$ mostly at temperatures above 22 °C and N:P higher than 100 (Fig. 4f). The highest C_f values were associated with N:P ratios of roughly 16 and temperatures of 20–24 °C (Fig. 4c). In contrast, relatively high C_p values were estimated at around 18 °C and between 25 and 28 °C when N:P ratios are low and at temperatures upon 18 °C when N:P ratios are high (Fig. 4f). The implication of the model is that the interaction of temperature and the relative concentration of nutrients plays an important role in the outcome of competition between fucoxanthin-containing phytoplankton and peridinin-containing dinoflagellates in the ECS.

3.4. Relations of the C_p/C_f ratio to interactions of temperature and nutrient stoichiometry

The C_p/C_f ratio showed higher values at ~18 °C and at above 26 °C (Fig. 5). There was a clear interaction between temperature and PO_4 concentration (Fig. 5a). A negative correlation was found between temperature and the C_p/C_f ratio at PO_4 concentrations greater than 0.8 μmol L^{-1}. At PO_4 concentrations between 0.4 μmol L^{-1} and 0.8 μmol L^{-1} there was a positive correlation between temperature and the C_p/C_f ratio. At PO_4 concentrations less than 0.4 μmol L^{-1} there was a minimum of the C_p/C_f ratio at intermediate temperatures. The ratio became higher at lower/higher temperature end members. The C_p/C_f ratio was also correlated with the interaction of temperature and NO_x concentration. It is clear that the higher ratios at ~18 °C occurred at NO_x concentrations ranging from 1 to 5 μmol L^{-1}, and the higher ratios at higher extreme temperatures occurred at NO_x concentrations less than 5 μmol L^{-1} (Fig. 5b). The implication is that the succession of fucoxanthin-containing phytoplankton and peridinin-containing dinoflagellates do depend on the absolute concentration of the limiting nutrient, while which nutrient is limiting depends on the ambient N:P ratio.

Based on the relationships between the C_p/C_f ratio and the interactions of temperature and nutrient concentrations, we formulated a GLM model (equation (3), Table S4). This model accounted for 97% of the variance of the C_p/C_f ratio, with the residuals showing no heterogeneity with respect to temperature (Fig. S5). Then we simulated the relationship of the C_p/C_f ratio and temperature at three constant PO_4 concentrations, 0.05 μmol L^{-1}, 0.25 μmol L^{-1}, and 0.6 μmol L^{-1}, based on this model. When we assumed the molar N:P ratio to be constant and equal to 16:1, the simulations presumably reflected the trends in the actual data at PO_4 concentrations less than 0.25 μmol L^{-1}, but deviated from the actual data at higher PO_4 concentrations (Fig. 5a and Fig. S6a). We therefore assumed that the N:P ratio varied from 8 to 32. Comparing with the actual data, we found that different temperatures selected for different optimum N:P ratios; lower temperature selected for a higher N:P ratio, whereas higher temperature selected for a lower N:P ratio (Fig. S6b). The explanation is that in the ocean the dissolved N:P ratio is not constant. The data showed that the NO_x concentration was positively correlated with the PO_4 concentration, and N:P ratio variability was dependent on both the PO_4 concentration and the temperature (Fig. S4a,b). We therefore calculated NO_x from PO_4 and temperature through equation (4) and repeated the simulations (Fig. 6).

3.5. Future responses of C_f and C_p to warming and eutrophication

Future changes in the C_f and C_p as a result of warming and eutrophication are not straightforward to anticipate because the effects of temperature, nutrients, and their interaction are all significant. Because we obtained clear relationships of the interaction of temperature and N:P ratio to C_f and C_p, using GAMM models F6 and P6 (Table S2), we simulated surface C_f and C_p concentrations based on assumed surface temperatures increases of 2 °C and N:P ratio increases of $e^2 = 7.4$ while leaving other parameters constant. The predicted C_f concentrations decreased significantly (*t*-test,

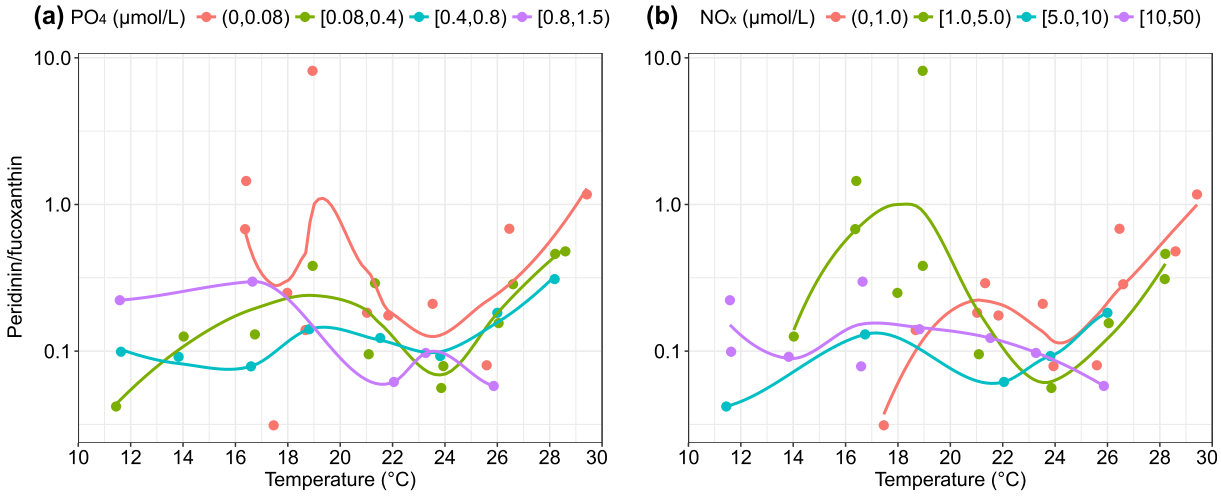

Fig. 5. Relationships of the peridinin/fucoxanthin ratio and temperature at different nutrient concentrations. The colored lines are simulated using the loess method (span = 0.7). **a.** Data were grouped by PO_4 concentration. **b.** Data were grouped by NO_x concentration. (For interpretation of the references to colur in this figure legend, the reader is referred to the web version of this article.)

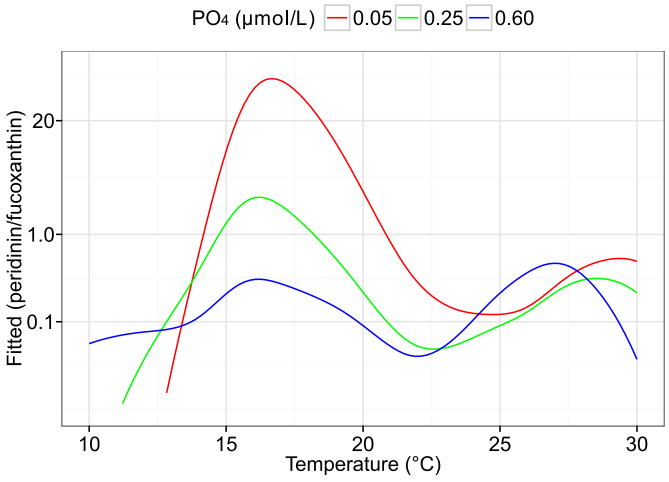

Fig. 6. Fitted ratio of peridinin/fucoxanthin on the basis of equation (3) at constant PO_4 concentrations. NO_x concentrations were calculated from PO_4 and temperature according to equation (4).

$p < 0.05$), with 60% stations showing decreased concentrations (Fig. 7a). In contrast, the predicted C_p increased significantly (*t*-test, $p < 0.05$), with 70% of the stations showing an increase (Fig. 7b). The magnitude of these changes was a function of latitude and longitude. Most of the big changes occurred in coastal regions, especially at the mouth of the Changjiang River estuary and adjacent coastal waters. The changes decreased in magnitude in a southeast offshore direction (Fig. 7).

We then focused on the surface waters of coastal regions with salinities less than 31. We predicted a significant decrease of C_f (Fig. 8a) and a significant increase of C_p (Fig. 8b) when temperature and ln N:P ratio were simultaneously increased by 0.25 °C and 0.25, respectively. The present surface median temperature and N:P ratio in these regions are 23.0 °C and $e^{3.19} = 24$, respectively. Given an increase of 2 units, the values would increase to 25 °C and $e^{5.19} = 180$ (~7 fold increase), respectively. Correspondingly, we predicted that the mean C_f should decrease by 19% (from 508 ng L^{-1} to 412 ng L^{-1}) while the mean C_p should increase by 60% (from 334 ng L^{-1} to 535 ng L^{-1}).

4. Discussion

Phytoplankton that contain peridinin are found only in the class Dinophyceae (Roy et al., 2011). Although not all autotrophic Dinophyceae contain peridinin (Zapata et al., 2012), the dominant species, *Prorocentrum donghaiense*, *Alexandrium catenella*, *Alexandrium minutum* and *Gymnodinium catenatum*, in the ECS do contain (Guo et al., 2014; Zapata et al., 2012). Fucoxanthin (*fuco*), however, is found in phytoplankton belonging to at least some species in five phytoplankton classes: Chrysophyceae, Pelagophyceae, Prymnesiophyceae, Bacillariophyceae, and Dinophyceae (Roy et al., 2011). Fucoxanthin is commonly associated with diatoms (i.e., Bacillariophyceae) (Letelier et al., 1993), but the presence in some of our samples of pigments such as 19′-butanoyloxyfucoxanthin (*but*) and 19′-hexanoyloxyfucoxanthin (*hex*), which are not associated with diatoms but are found in some species of Pelagophyceae, Prymnesiophyceae, and Dinophyceae, indicates that diatoms did not account for all the fucoxanthin in our samples. However, the *fuco*/*but* and *fuco*/*hex* ratios in our samples averaged 15 and 6, respectively, whereas the *fuco*/*but* and *fuco*/*hex* ratios in Dinophyceae and Prymnesiophyceae, for example, are only about 0.5 and 0.02, respectively (Chang and Gall, 2013; Letelier et al., 1993), thus it seems unlikely that the fucoxanthin in our samples reflects high biomass of Dinophyceae and Prymnesiophyceae. We do have some cases where the concentrations of *but* and *hex* exceed the fucoxanthin concentrations. Those cases presumably are Chrysophyceae, Prymnesiophyceae, Pelagophyceae, and maybe some of the Dinophyceae that contain no peridinin. However, those are all cases where the fucoxanthin concentrations are low (Fig. S7). Another possible source of fucoxanthin may be Phaeophyta, but

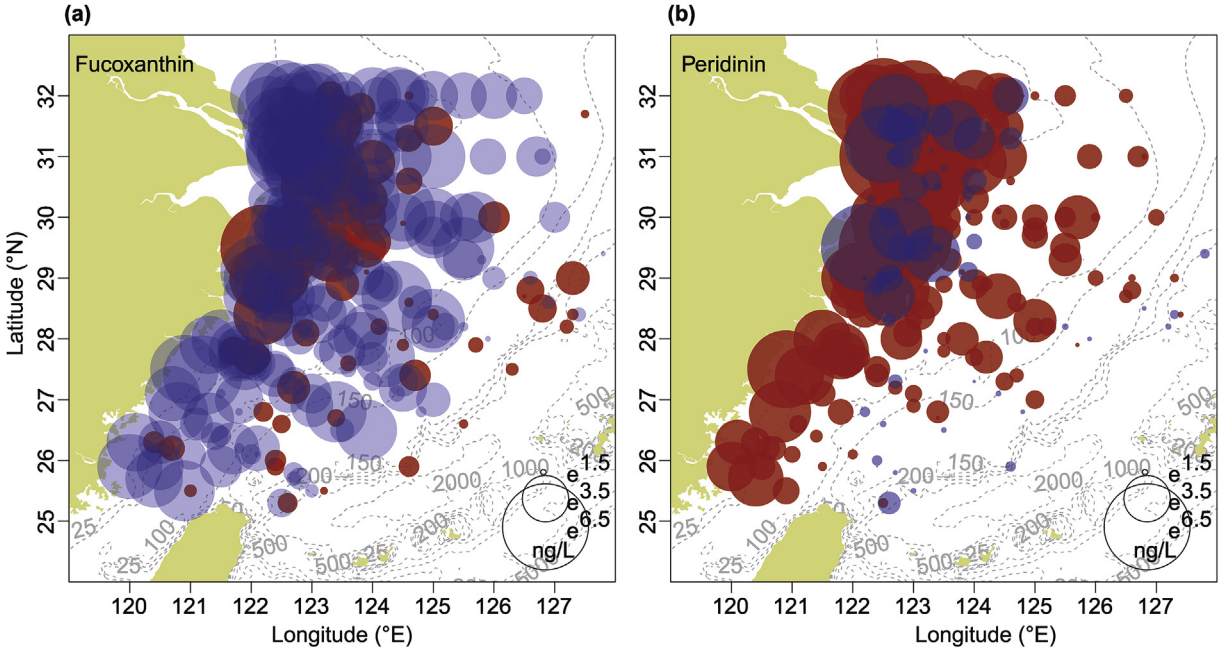

Fig. 7. Distribution of predicted changes in pigment concentrations assuming surface temperatures increases of 2 °C and N:P ratio increases of $e^2 = 7.4$. Red circles represent increases and blue circles decreases compared to present concentrations. **a.** fucoxanthin. **b.** peridinin. (For interpretation of the references to colour in this figure legend, the reader is referred to the web version of this article.)

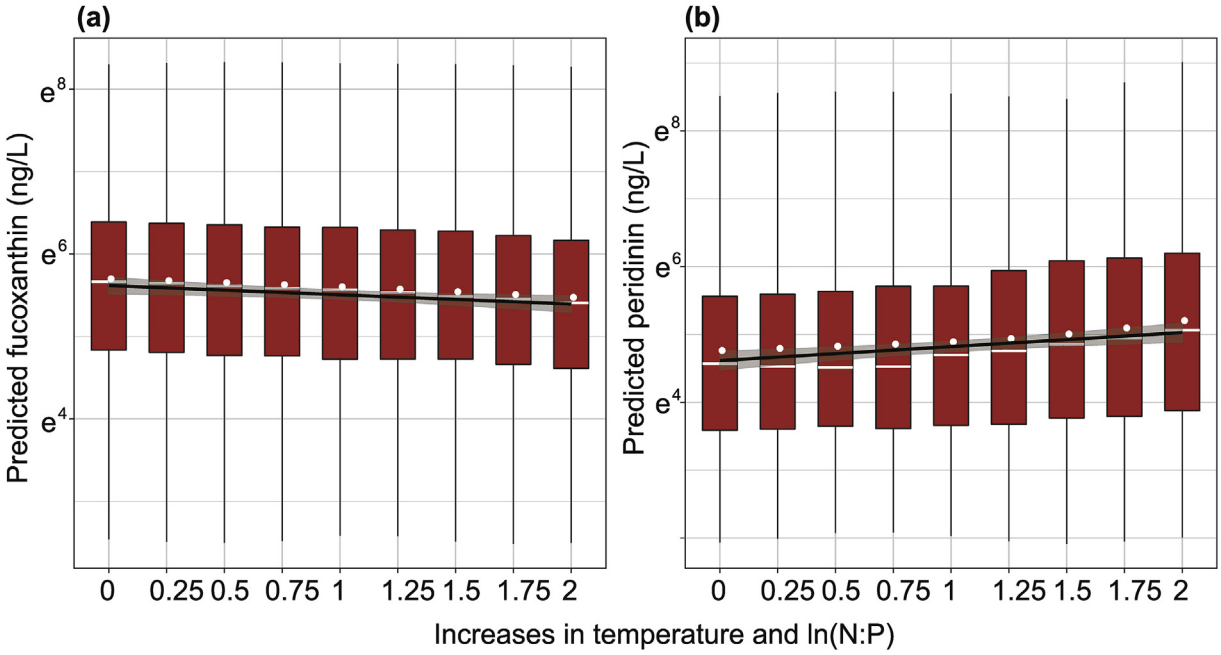

Fig. 8. Predicted concentrations of pigments displayed as a boxplot for a sequence of increases in both temperature and ln transformed N:P ratio. The white horizontal line and the white dot inside each box are the median and the mean respectively. The solid line across the boxes represents GAM smoothing and shaded areas denote 95% confidence bands. **a.** fucoxanthin. **b.** peridinin.

such macroalgae are usually benthic and unlikely to be contained in our water samples. In our previous study, diagnostic pigment concentration in the ECS was comparable to the microscopy results based on morphology (Liu et al., 2016). Thus we feel confident in assuming that most of the fucoxanthin and peridinin in our samples was associated with diatoms and dinoflagellates, respectively, and that all of the high fucoxanthin concentrations were the result of diatom blooms.

Based on the raw data, our GAMM model revealed that C_f exceeded C_p in the ECS when NO_x and PO_4 concentrations were relatively high (Fig. 3c,e). The C_p concentrations were relatively high when PO_4 concentrations were less than 0.1 μmol L^{-1} but NOx concentrations were higher than 0.5 μmol L^{-1} (Fig. 3d,f). These patterns in fact seem reasonable if we assume that most of the fucoxanthin was associated with diatoms. Diatoms tend to have a competitive advantage when nutrient concentrations are high for several reasons. Diatoms are typically *R*-strategists (species tolerant of shear/stress forces in physically disturbed water masses) (Alves-de-Souza et al., 2008) and tend to have high maximum carbon-specific nutrient uptake rates and disproportionately large storage vacuoles (Edwards et al., 2012; Litchman and Klausmeier, 2008). Dinoflagellates, however, may replace diatoms by using multiple growth strategies (*C*, colonist species which predominate in chemically disturbed habitats; *S*, nutrient stress tolerant species; and *R*) to exploit abiotic habitats that support them (Smayda and Reynolds, 2003). Dinoflagellate have an intrinsically high affinity for phosphate and the ability to utilize organic phosphorus compounds via alkaline phosphatase (e.g., *P. donghaiense*) (Huang et al., 2005), as well as mixotrophic and vertical migration capabilities. As a group, dinoflagellates are not very sensitive to nutrient conditions.

We found that lower temperatures favored diatoms and that higher temperatures inhibited the growth of diatoms. That dinoflagellates were less sensitive to temperature than diatoms (Fig. 3a and b) is inconsistent with a previous found that the adaptive temperature range of diatoms (*Skeletonema costatum*, 15–25 °C) is wider than that of dinoflagellates (*P. donghaiense*, 20–25 °C) (Wang et al., 2006) and the global scenario that diatoms have a wider thermal tolerance than dinoflagellates (Chen, 2015). However, we found that the temperature effect was very dependent on the nutrient regime, a consequence of either species specific variations or an interact effect of the temperature and the nutrient regime on the same dominant species. The result showed that diatoms can tolerate higher temperatures at high nutrient (NO_x and PO_4) concentrations than at low nutrient concentrations (Fig. 4a,c). The implication is that the response of diatoms to high temperature may not be a consequence of an inherent metabolic intolerance to supraoptimal temperatures as long as the temperature stress is not accompanied by the additional stress of nutrient limitation. Thermal stratification of marine waters will increase as a consequence of global warming, which will inhibit nutrient inputs from waters below the mixed layer. In the offshore waters of the ECS, a reduced degree of mixing in the summer results in low nutrient availability, which inhibits the growth of diatoms but has no apparent negative effect on *S*-strategist dinoflagellate species. Such species include the harmful unarmored dinoflagellate *Cochlodinium polykrikoides*, which prefers a temperature of ~27 °C (Matsuoka et al., 2010). In the coastal waters, there is a continuous input of terrestrial nutrients from the Changjiang River, even when the seawater is stratified, and that input benefits diatoms (Furuya et al., 2003). High nutrient concentrations that benefit diatoms also occur in the Changjiang Diluted Water front, where it mixes with the Taiwan Warm Current Water, and in the upwelling zones in the coastal waters of Zhejiang and Fujian provinces (Tang et al., 2006), where diatom blooms have been reported. However, dinoflagellates may replace diatoms in any of these areas if there is a relaxation of the processes that deliver the allochthonous nutrients (Smayda, 2010). For example, well-known late spring dinoflagellate blooms (*Gymnodinium* and *Prorocentrum* species) occur at temperatures of ~18 °C when nutrient concentrations are low, after the phosphate has been consumed by diatoms and there is still some nitrogen remaining. This phenomenon has been reported in the

ECS (Guo et al., 2014) and in other coastal and shelf areas (Anderson et al., 2002; Heisler et al., 2008). Similarly, we found that during the summer Changjiang Diluted Water, characterized by both high temperatures and high nutrient concentrations, can be a site of dinoflagellate blooms (Fig. 4d–f), perhaps due to the combined ability of *R*- and *S*-strategists to tolerate high turbulence and phosphate depletion, but otherwise eutrophic conditions. The biomass of diatoms relative to that of dinoflagellates decreased from 1959 to 2009 in the Changjiang River estuary and adjacent coastal waters in summer (Jiang et al., 2014). Our data (Fig. 2) and model results indicate that this pattern may have been enhanced in the past several years.

Using surface microscopy data (dominated by *Pseudo-nitzschia delicatissima*, *Thalassionema nitzschioides*, *Paralia sulcata*, and *Skeletonema* sp. for diatoms, and *P. donghainese*, *Scrippsiella trochoidea*, and *G. lohmanni* for dinoflagellates) collected from cruises C1–C4 (Table S1), Guo et al. (2014) has obtained a decreasing trend for diatoms against N:P ratio and an opposite trend for dinoflagellates against N:P ratio. Our analysis of temperature and N:P ratios provides additional insight into the dynamics of diatoms and dinoflagellates in the ECS. An analysis of the GAMM results (Fig. 4) and an analysis of the medians of the bins of the GLM results (Figs. 5 and 6) revealed that the N:P ratio may be a factor that drives the succession of diatoms and dinoflagellates, and that the effect of the N:P ratio is a function of temperature. The N:P ratio in algal biomass is positively correlated with temperature at the global scale (Yvon-Durocher et al., 2015), and the external N:P ratio is negatively correlated with temperature in the ECS (Fig. S4b). The implication is that the algal internal N:P ratio will exceed the external N:P ratio when the temperature is higher than a threshold. Because the internal N:P ratio of dinoflagellates is generally higher than that of diatoms (John and Flynn, 2000; Rhee and Gotham, 1981), the high N:P ratios of particulate matter at high temperatures was probably accounted for by the greater biomass of dinoflagellates, the indication being that high temperatures favor dinoflagellates in the ECS. In addition, according to the resource ratio theory (Rhee and Gotham, 1981; Tilman, 1977), if the maximum growth rates of diatoms and dinoflagellates are similar, diatoms will competitively eliminate dinoflagellates when external N:P ratios are low, whereas mixotrophic dinoflagellates will prevail when the external N:P ratios are high. Given the fact that dinoflagellates typically have lower growth rates than do diatoms of a comparable size (Finkel et al., 2010), the internal N:P ratio must be lower for diatoms than dinoflagellates (Klausmeier et al., 2004a, 2004b). The winner of the competition will therefore tend to be mixotrophic dinoflagellates when the external N:P ratios are high, a conclusion consistent with our observations that high N:P ratios favor dinoflagellates in the ECS and a previous report that a high N:P condition is more likely to promote species that have slow growth rates (Glibert and Burkholder, 2011). The N:P ratio (26 ± 20) at PO_4 concentrations less than 0.08 μmol L^{-1} was obviously higher than the N:P ratio (17 ± 8) at higher PO_4 concentrations. The ratio of C_p/C_f was significantly higher for PO4 < 0.08 μmol L^{-1} than at the latter conditions (Kruskal-Wallis rank sum test, $p < 0.001$, Fig. S4c). Because there is evidence that the internal N:P ratio is highest under phosphorus limited conditions compared to the condition of abundant resources and conditions limited by light or nitrogen (Klausmeier et al., 2004a), the dominance of dinoflagellate under high N:P conditions is expected in the ECS.

The GLM model reflected the fact that the spring dinoflagellate blooms became weaker with increasing PO_4 concentrations but became stronger with increasing N:P ratios (Fig. 6 and Fig. S6b). Projecting future changes of these blooms requires knowing what will happen to nutrient concentrations as a result of eutrophication. Assuming a C/Chl*a* ratio of 50 by weight and a C/N ratio of 5.68 by weight (Laws, 1991; Laws and Redalje, 1979; Laws and Wong, 1979), we estimated that the percentage of nitrogen in phytoplankton was negatively correlated with nutrient concentrations, and this relationship was rather insensitive to the assumed C/Chl*a* and C/N ratio (Fig. S8). Therefore, low ambient nutrient concentrations were the result of phytoplankton taking up a large fraction of the nutrients. In accord with this logic, we hypothesized that there would be an increase in phytoplankton as a result of eutrophication instead of an increase of inorganic nutrient concentrations. Previous studies have demonstrated that the nitrogen in the ECS has been increasing while the phosphorus has been decreasing slightly as a result of the long-term increase in the Changjiang River discharge and an increase in nitrogen fertilizer use in China (Jiang et al., 2014; Zhou et al., 2008). The regression lines between NO_x and PO_4 would therefore move toward the left and up (Fig. S4a). The result would be more phosphate-limited situations, leading to higher N:P ratios, and such conditions would favor dinoflagellates.

To predict the future responses of diatom and dinoflagellate biomass to combined effects of warming and eutrophication, we assumed a 2 °C increase in water temperatures and ~7.4-fold increase in the N:P ratio and focused on the surface water of coastal regions with salinity less than 31 (Gong et al., 1996). The surface waters of the ECS underwent a significant warming at a rate of 0.09 °C per decade during 1870–2011 (Bao and Ren, 2014). The largest warming trend occurred in the mouth of the Changjiang River, where the annual mean warming rate exceeded 2.4 °C per century (Liu and Zhang, 2013) and exceeded 0.49 °C per decade in the summer (Jiang et al., 2014). If this warming trend continues, it is reasonable to assume that there will be a temperature rise of at least 2 °C by 2100 in the surface waters of much of the ECS. In addition to warming, anthropogenic activities have led to a shift in the nutrient regime in the ECS, especially in the Changjiang River estuary and adjacent coastal waters, where the N:P ratio has been steadily increasing (Zhou et al., 2008), and the observed average molar N:P ratio in 2010 reached about 200 (Jiang et al., 2014). As a result of the increase of nitrogen fertilizer use in China, our presumptive future N:P ratio of about 180 will therefore likely be an underestimate, at least near the Changjiang River estuary. We predict that the mean C_f should decrease by 19% and the mean C_p should increase by 60% as the temperature increases by 2 °C. These decrease in C_f and increase in C_p reflect a shift from diatoms to dinoflagellates over the next century, as proposed previously (Jiang et al., 2014; Zhou et al., 2008). We did not project changes of temperature beyond the year 2100 because it is unclear whether phytoplankton will adapt to future niches over time (Irwin et al., 2015). Changes beyond 2100 could have even more serious implications than the changes we have projected. We did not project changes of N:P ratio over 180 because such situations may be more complicated than we assumed here. For instance, although silicate is not limiting in the ECS at present, increasing nitrogen input and diatom consumption will result in a decrease of Si:N ratio (Jiang et al., 2014), and silicate may be the limiting factor for diatoms someday.

It is important to realize that the influence of changes in irradiance may alter phytoplankton community composition (Barton et al., 2015; Edwards et al., 2015), but we do not feel that the predictions of our model are seriously compromised by the absence of irradiance because the indirect effect of this factor is accounted for approximately by the variables we considered in this study; temperature, irradiance, nutrient concentrations and ratios and changes in these variables co-vary (Irwin et al., 2012; Litchman and Klausmeier, 2008). An important caveat is that we did not consider the effect of grazing because high-resolution sampling of processes such as grazing is difficult. Because observations in the China seas have shown that microzooplankton grazing is enhanced in

eutrophic ecosystems (Chen et al., 2012; Zheng et al., 2015), further study is needed to explore the effect of grazing to make more realistic predictions about the impact of future climate scenarios.

5. Conclusions

We determined a series of quantitative functional responses of diatom and dinoflagellate biomass (C_f and C_p) resulting from the interaction of temperature and nutrient concentrations or ratios. Such interaction is key in driving the succession of diatoms and dinoflagellates in the ECS. We project that decreases in diatom biomass (C_f) of 19% should occur in 60% of stations while increases in dinoflagellate biomass (C_p) of 60% should occur in 70% of stations as a result of anthropogenic changes in temperature and nutrient inputs. Such a shift projects a more important role of dinoflagellates in this coastal ecosystem, including a change in the timing and increase in the spatial extent and frequency of dinoflagellate blooms. These changes may be responsible for a decrease of fish production and an increase of gelatinous organisms, such as jellyfish in the ECS (Jiang et al., 2008). Because the sinking rate of dinoflagellates is lower than that of diatoms (Guo et al., 2015), these changes may also reduce the efficiency of the biological pump in the ECS. Such a shift in phytoplankton community structure from diatoms to dinoflagellates should be taken into consideration in future studies of global climate models, carbon cycling and fishery yields.

Acknowledgements

This work was supported by grants from the National Key Research and Development Program of China (No.2016YFA0601201), the China NSF (Nos. 41406143, 41330961, U1406403), the Chinese Academy of Science Project (XDA11020103) and China Postdoctoral Science Foundation funded project (2014M551839). We thank Profs. Sumei Liu, Minhan Dai, Zhigang Yu and Zhiming Yu for nutrient data, and Profs. Daji Huang, Jianyu Hu, Hao Wei and Fei Yu for hydrographic data. We also thank Michael R. Landry and Paul J. Harrision for their helpful comments and suggestions on this manuscript.

Appendix A. Supplementary data

Supplementary data related to this article can be found at https://doi.org/10.1016/j.watres.2017.10.051.

References

Agusti, S., Vaqué, D., Estrada, M., Cerezo, M.I., Salazar, G., Gasol, J.M., Duarte, C.M., 2014. Ubiquitous healthy diatoms in the deep sea confirm deep carbon injection by the biological pump. Nat. Commun. 6, 6–7608.
Alves-de-Souza, C., González, M.T., Iriarte, J.L., 2008. Functional groups in marine phytoplankton assemblages dominated by diatoms in fjords of southern Chile. J. Plankton Res. 30 (11), 1233–1243.
Anderson, D.M., Glibert, P.M., Burkholder, J.M., 2002. Harmful algal blooms and eutrophication: nutrient sources, composition, and consequences. Estuaries 25 (4), 704–726.
Bao, B., Ren, G., 2014. Climatological characteristics and long-term change of SST over the marginal seas of China. Cont. Shelf Res. 77, 96–106.
Barton, A.D., Irwin, A.J., Finkel, Z.V., Stock, C.A., 2016. Anthropogenic climate change drives shift and shuffle in North Atlantic phytoplankton communities. Proc. Natl. Acad. Sci. 113 (11), 2964–2969.
Barton, A.D., Lozier, M.S., Williams, R.G., 2015. Physical controls of variability in North Atlantic phytoplankton communities. Limnol. Oceanogr. 60 (1), 181–197.
Chang, F.H., Gall, M., 2013. Pigment compositions and toxic effects of three harmful *Karenia* species, *Karenia concordia, Karenia brevisulcata* and *Karenia mikimotoi* (Gymnodiniales, Dinophyceae), on rotifers and brine shrimps. Harmful Algae 27 (3), 113–120.
Chen, B., 2015. Patterns of thermal limits of phytoplankton. J. Plankton Res. 37 (2), 285–292.
Chen, B., Landry, M.R., Huang, B., Liu, H., 2012. Does warming enhance the effect of microzooplankton grazing on marine phytoplankton in the ocean? Limnol. Oceanogr. 57 (2), 519–526.
Doney, S.C., Ruckelshaus, M., Duffy, J.E., Barry, J.P., Chan, F., English, C.A., Galindo, H.M., Grebmeier, J.M., Hollowed, A.B., Knowlton, N., 2012. Climate change impacts on marine ecosystems. Annu. Rev. Mar. Sci. 4 (1), 11–37.
Edwards, K.F., Thomas, M.K., Klausmeier, C.A., Litchman, E., 2012. Allometric scaling and taxonomic variation in nutrient utilization traits and maximum growth rate of phytoplankton. Limnol. Oceanogr. 57 (2), 554–566.
Edwards, K.F., Thomas, M.K., Klausmeier, C.A., Litchman, E., 2015. Light and growth in marine phytoplankton: allometric, taxonomic, and environmental variation. Limnol. Oceanogr. 60 (2), 540–552.
Edwards, M., Johns, D.G., Leterme, S.C., Svendsen, E., Richardson, A.J., 2006. Regional climate change and harmful algal blooms in the northeast Atlantic. Limnol. Oceanogr. 51 (2), 820–829.
Edwards, M., Richardson, A.J., 2004. Impact of climate change on marine pelagic phenology and trophic mismatch. Nature 430 (7002), 881–884.
Finkel, Z.V., Beardall, J., Flynn, K.J., Quigg, A., Rees, T.A.V., Raven, J.A., 2010. Phytoplankton in a changing world: cell size and elemental stoichiometry. J. Plankton Res. 32 (1), 119–137.
Furuya, K., Hayashi, M., Yabushita, Y., Ishikawa, A., 2003. Phytoplankton dynamics in the East China Sea in spring and summer as revealed by HPLC-derived pigment signatures. Deep Sea Res. Part II Top. Stud. Oceanogr. 50 (2), 367–387.
Glibert, P.M., Allen, J.I., Bouwman, A.F., Brown, C.W., Flynn, K.J., Lewitus, A.J., Madden, C.J., 2010. Modeling of HABs and eutrophication: status, advances, challenges. J. Mar. Syst. 83 (3), 262–275.
Glibert, P.M., Burkholder, J.A.M., 2011. Harmful algal blooms and eutrophication: "strategies" for nutrient uptake and growth outside the Redfield comfort zone. Chin. J. Oceanol. Limnol. 29 (4), 724–738.
Gong, G., Lee Chen, Y., Liu, K., 1996. Chemical hydrography and chlorophyll *a* distribution in the East China Sea in summer: implications in nutrient dynamics. Cont. Shelf Res. 16 (12), 1561–1590.
Guo, S., Feng, Y., Wang, L., Dai, M., Liu, Z., Bai, Y., Sun, J., 2014. Seasonal variation in the phytoplankton community of a continental-shelf sea: the East China Sea. Mar. Ecol. Prog. Ser. 516, 103–126.
Guo, S., Sun, J., Zhao, Q., Feng, Y., Huang, D., Liu, S., 2015. Sinking rates of phytoplankton in the Changjiang (Yangtze River) estuary: a comparative study between *Prorocentrum dentatum* and *Skeletonema dorhnii* bloom. J. Mar. Syst. 154, 5–14.
Hallegraeff, G.M., 2010. Ocean climate change, phytoplankton community responses, and harmful algal blooms: a formidable predictive challenge. J. Phycol. 46 (2), 220–235.
Han, A., Dai, M., Kao, S., Gan, J., Li, Q., Wang, L., Zhai, W., Wang, L., 2012. Nutrient dynamics and biological consumption in a large continental shelf system under the influence of both a river plume and coastal upwelling. Limnol. Oceanogr. 57 (2), 486–502.
Heisler, J., Glibert, P.M., Burkholder, J.M., Anderson, D.M., Cochlan, W., Dennison, W.C., Dortch, Q., Gobler, C.J., Heil, C.A., Humphries, E., 2008. Eutrophication and harmful algal blooms: a scientific consensus. Harmful Algae 8 (1), 3–13.
Hinder, S.L., Hays, G.C., Edwards, M., Roberts, E.C., Walne, A.W., Gravenor, M.B., 2012. Changes in marine dinoflagellate and diatom abundance under climate change. Nat. Clim. Change 2 (4), 271–275.
Huang, B., Ou, L., Hong, H., Luo, H., Wang, D., 2005. Bioavailability of dissolved organic phosphorus compounds to typical harmful dinoflagellate *Prorocentrum donghaiense* Lu. Mar. Pollut. Bull. 51 (8), 838–844.
Irwin, A.J., Finkel, Z.V., Müller-Karger, F.E., Ghinaglia, L.T., 2015. Phytoplankton adapt to changing ocean environments. Proc. Natl. Acad. Sci. 112 (18), 5762–5766.
Irwin, A.J., Nelles, A.M., Finkel, Z.V., 2012. Phytoplankton niches estimated from field data. Limnol. Oceanogr. 57 (3), 787–797.
Jiang, H., Cheng, H.-Q., Xu, H.-G., Arreguín-Sánchez, F., Zetina-Rejón, M.J., Luna, P.D.M., Le Quesne, W.J.F., 2008. Trophic controls of jellyfish blooms and links with fisheries in the East China Sea. Ecol. Model. 212 (3), 492–503.
Jiang, Z., Liu, J., Chen, J., Chen, Q., Yan, X., Xuan, J., Zeng, J., 2014. Responses of summer phytoplankton community to drastic environmental changes in the Changjiang (Yangtze River) estuary during the past 50 years. Water Res. 54, 1–11.
John, E.H., Flynn, K.J., 2000. Growth dynamics and toxicity of *Alexandrium fundyense* (Dinophyceae): the effect of changing N: P supply ratios on internal toxin and nutrient levels. Eur. J. Phycol. 35 (1), 11–23.
Karl, T.R., Trenberth, K.E., 2003. Modern global climate change. Science 302 (5651), 1719–1723.
Klausmeier, C.A., Litchman, E., Daufresne, T., Levin, S.A., 2004a. Optimal nitrogen-to-phosphorus stoichiometry of phytoplankton. Nature 429 (6988), 171–174.
Klausmeier, C.A., Litchman, E., Levin, S.A., 2004b. Phytoplankton growth and stoichiometry under multiple nutrient limitation. Limnol. Oceanogr. 49 (4), 1463–1470.
Laws, E.A., 1991. Photosynthetic quotients, new production and net community production in the open ocean. Deep Sea Res. Part A Oceanogr. Res. Pap. 38 (1), 143–167.
Laws, E.A., Redalje, D.G., 1979. Effect of sewage enrichment on the phytoplankton population of a subtropical estuary. Pacificence 33 (2), 129–144.
Laws, E.A., Wong, D.C.L., 1979. Studies of carbon and nitrogen metabolism by three marine phytoplankton species in nitrate-limited continuous culture. J. Phycol. 14 (4), 406–416.
Letelier, R.M., Bidigare, R.R., Hebel, D.V., Ondrusek, M., Winn, C.D., Karl, M., 1993.

Temporal variability of phytoplankton community structure based on pigment analysis. Limnol. Oceanogr. 38 (7), 1420–1437.
Leterme, S.C., Edwards, M., Seuront, L., Attrill, M.J., Reid, P.C., John, A.W.G., 2005. Decadal basin-scale changes in diatoms, dinoflagellates, and phytoplankton color across the North Atlantic. Limnol. Oceanogr. 50 (4), 1244–1253.
Leterme, S.C., Seuront, L., Edwards, M., 2006. Differential contribution of diatoms and dinoflagellates to phytoplankton biomass in the NE Atlantic Ocean and the North Sea. Mar. Ecol. Prog. Ser. 312 (8), 57–65.
Lewandowska, A.M., Boyce, D.G., Hofmann, M., Matthiessen, B., Sommer, U., Worm, B., 2014. Effects of sea surface warming on marine plankton. Ecol. Lett. 17 (5), 614–623.
Litchman, E., Klausmeier, C.A., 2008. Trait-based community ecology of phytoplankton. Annu. Rev. Ecol. Evol. Syst. 615–639.
Liu, Q., Zhang, Q., 2013. Analysis on long-term change of sea surface temperature in the China Seas. J. Ocean Univ. China 12 (2), 295–300.
Liu, X., Huang, B., Liu, Z., Wang, L., Wei, H., Li, C., Huang, Q., 2012. High-resolution phytoplankton diel variations in the summer stratified central Yellow Sea. J. Oceanogr. 68 (6), 913–927.
Liu, X., Xiao, W., Landry, M.R., Chiang, K.-P., Wang, L., Huang, B., 2016. Responses of phytoplankton communities to environmental variability in the East China Sea. Ecosystems 1–18.
Margalef, R., 1977. Life-Forms of phytoplankton as survival alternatives in an unstable environment. Oceanologia 1 (4), 493–509.
Matsuoka, K., Mizuno, A., Iwataki, M., Takano, Y., Yamatogi, T., Yoon, Y.H., Lee, J.-B., 2010. Seed populations of a harmful unarmored dinoflagellate *Cochlodinium polykrikoides* Margalef in the East China Sea. Harmful Algae 9 (6), 548–556.
Menden-Deuer, S., Lessard, E.J., 2000. Carbon to volume relationships for dinoflagellates, diatoms, and other protist plankton. Limnol. Oceanogr. 45 (3), 569–579.
Moore, S.K., Trainer, V.L., Mantua, N.J., Parker, M.S., Laws, E.A., Backer, L.C., Fleming, L.E., 2008. Impacts of climate variability and future climate change on harmful algal blooms and human health. Environ. Health 7. Suppl 2(Suppl2), S4–S4.
Peloquin, J., Swan, C., Gruber, N., Vogt, M., Claustre, H., Ras, J., Uitz, J., Barlow, R., Behrenfeld, M., Bidigare, R., 2013. The MAREDAT global database of high performance liquid chromatography marine pigment measurements. Earth Syst. Sci. Data 5 (1), 109–123.
Reynolds, C.S., 1987. The response of phytoplankton communities to changing lake environments. Aquat. Sci. 49 (2), 220–236.
R Development Core Team, 2016. R: a Language and Environment for Statistical Computing. Vienna, Austria: R Foundation for Statistical Computing. Open access available at: http://cran.r-project.org.
Rhee, G.Y., Gotham, I.J., 1981. Optimum N: P ratios and coexistence of planktonic algae. J. Phycol. 16 (4), 486–489.
Roy, S., Llewellyn, C.A., Egeland, E.S., Johnsen, G., 2011. Phytoplankton Pigments: Characterization, Chemotaxonomy and Applications in Oceanography. Cambridge University Press.
Smayda, T., 2010. Adaptations and selection of harmful and other dinoflagellate species in upwelling systems. 2. Motility and migratory behaviour. Prog. Oceanogr. 85 (1), 71–91.
Smayda, T.J., Reynolds, C.S., 2001. Community assembly in marine phytoplankton: application of recent models to harmful dinoflagellate blooms. J. Plankton Res. 23 (5), 447–461.
Smayda, T.J., Reynolds, C.S., 2003. Strategies of marine dinoflagellate survival and some rules of assembly. J. Sea Res. 49 (2), 95–106.
Tang, D., Di, B., Wei, G., Ni, I.-H., Wang, S., 2006. Spatial, seasonal and species variations of harmful algal blooms in the South Yellow Sea and East China Sea. Hydrobiologia 568 (1), 245–253.
Tilman, D., 1977. Resource competition between plankton algae: an experimental and theoretical approach. Ecology 58 (2), 338–348.
Wang, Z., Li, R., Zhu, M., 2006. Study on population growth processes and interspecific competition of *Prorocentrum donghaiense* and *Skeletonema costatum* in semi-continuous dilution experiments. Adv. Mar. Sci. 24, 496–503. https://doi.org/10.3969/j.issn.1671-6647.2006.04.011 (Article in Chinese with English abstract).
Wells, M.L., Trainer, V.L., Smayda, T.J., Karlson, B.S., Trick, C.G., Kudela, R.M., Ishikawa, A., Bernard, S., Wulff, A., Anderson, D.M., 2015. Harmful algal blooms and climate change: learning from the past and present to forecast the future. Harmful Algae 49, 68–93.
Wood, S., 2006. Generalized Additive Models: an Introduction with R. Chapman and Hall.
Xie, Y., Tilstone, G.H., Widdicombe, C.L., Woodward, E.M.S., Harris, C., Barnes, M.K.S., 2015. Effects of increases in temperature and nutrients on phytoplankton community structure and photosynthesis in the Western English Channel. Mar. Ecol. Prog. Ser. 519, 61–73.
Yvon-Durocher, G., Dossena, M., Trimmer, M., Woodward, G., Allen, A.P., 2015. Temperature and the biogeography of algal stoichiometry. Glob. Ecol. Biogeogr. 24, 562–570.
Zapata, M., Fraga, S., Rodríguez, F., Garrido, J.L., 2012. Pigment-based chloroplast types in dinoflagellates. Mar. Ecol. Prog. Ser. 465, 33–52.
Zheng, L., Chen, B., Liu, X., Huang, B., Liu, H., Song, S., 2015. Seasonal variations in the effect of microzooplankton grazing on phytoplankton in the East China Sea. Cont. Shelf Res. 111, 304–315.
Zhou, M., Shen, Z., Yu, R., 2008. Responses of a coastal phytoplankton community to increased nutrient input from the Changjiang (Yangtze) River. Cont. Shelf Res. 28 (12), 1483–1489.
Zuur, A.F., Ieno, E.N., Walker, N.J., Saveliev, A.A., Smith, G.M., 2009. Mixed Effect Models and Extensions in Ecology with R. Springer, New York.